https://doi.org/10.5194/egusphere-2026-1761
Preprint. Discussion started: 23 June 2026

Title Page

Biochar addition enhances soil aggregate stability by modulating soil internal forces: The critical role of readily oxidized organic carbon and particulate organic carbon

Xiaoshuai Song[a,b,c], Chenyang Xu[d,e], Huanhuan Zhao[d], Jiangwen Li[a,b,f], Wei Du[d,e], Wuquan Ding[g], Zhenghong Yu[h], Fengbao Zhang[a,b,f], Feinan Hu[a,b,f]*

[a] State Key Laboratory of Soil and Water Conservation and Desertification Control, the Research Center of Soil and Water Conservation and Ecological Environment, Chinese Academy of Sciences and Ministry of Education, Yangling, Shaanxi 712100, China;

[b] Institute of Soil and Water Conservation, Chinese Academy of Sciences and Ministry of Water Resources, Yangling, Shaanxi 712100, China;

[c] University of Chinese Academy of Sciences, Beijing 100049, China;

[d] College of Natural Resources and Environment, Northwest A&F University, Yangling, Shaanxi 712100, China;

[e] Key Laboratory of Plant Nutrition and Agri-environment in Northwest China, Ministry of Agriculture and Rural Affairs, Yangling, Shaanxi 712100, China;

[f] College of Soil and Water Conservation Science and Engineering, Northwest A&F University, Yangling, Shaanxi 712100, China;

[g] Chongqing Key Laboratory of Environmental Materials & Remediation Technologies, Chongqing University of Arts and Science, Chongqing 402168, China;

[h] College of Desert Management, Inner Mongolia Agricultural University, Hohhot 010000, China.

***Corresponding author:** Feinan Hu, address: No. 26, Xi'nong Road, State Key

https://doi.org/10.5194/egusphere-2026-1761
Preprint. Discussion started: 23 June 2026

Laboratory of Soil and Water Conservation and Desertification Control, Northwest A&F University, Yangling, Shaanxi 712100, China; email: hufn@nwafu.edu.cn; telephone: +86-029-87011863; fax: +86-029-87010623.

https://doi.org/10.5194/egusphere-2026-1761
Preprint. Discussion started: 23 June 2026

Abstract: Degradation of soil structure and function is a significant obstacle to sustainable agriculture, yet using biochar is known to be an effective way of increasing soil organic carbon and boosting structure. Aggregate stability is greatly influenced by soil internal forces (SIFs), such as van der Waals, hydration, and electrostatic forces. However, it is still not clear which specific organic carbon components play a significant role in the stability of aggregates and the action of soil internal forces. In this study, a field simulation experiment was conducted using maize straw and wheat straw biochars to investigate how biochar addtion affect soil aggregate stability. The findings showed that as the rate of biochar application increased from 0% to 10% over 180 day and 365 days, the contents of soil light fraction organic carbon (LFOC), particulate organic carbon (POC), dissolved organic carbon (DOC), readily oxidized organic carbon (ROC), as well as soil specific surface area and surface charge number, increased. The content of different carbon fractions decreased with prolonged incubation time, while soil electrochemical parameters continued to increase throughout the incubation period. Pearson correlation and redundancy analyses showed that soil active organic carbon fractions were strongly correlated with soil surface electrochemical properties, with ROC and POC being the primary factors. Soil aggregate stability increased with higher biochar application rates, and the beneficial effect of biochar on aggregate stability became increasingly pronounced over time. Based on the quantitative estimates of SIFs, the addition of biochar facilitated soil aggregates stability by increasing van der Waals attractive pressure and decreasing electrostatic repulsive pressure, and finally lowering net

https://doi.org/10.5194/egusphere-2026-1761
Preprint. Discussion started: 23 June 2026

repulsive pressure between soil particles. The soil aggregate breaking strength increased quickly at initially and then leveled out as the electrolyte content decreased; 10^{-2} mol L^{-1} marked the tipping point. The study identified the active organic carbon (ROC and POC) fractions which could mediate the soil surface electrochemical properties and soil internal forces, finally enhance soil aggregate stability. Our research provides a theoretical basis for the targeted use and modifying of biochar to efficiently improve soil structure.

Keywords: Biochar; Active organic carbon fraction; Soil internal forces; Aggregate stability

1. Introduction

Soil structural stability is a key indicator for assessing soil erodibility, directly influencing the occurrence and evolution of soil erosion processes (An et al., 2010; Siedt et al., 2021). Soil aggregate formation and stabilization play a fundamental role in shaping soil architecture and underpin a wide range of soil functions (Batista et al., 2023; Li et al., 2016; Rabot et al., 2018). Physical characteristics like porosity, aeration, compaction, and water retention, as well as biochemical characteristics like organic carbon fixation, conversion, and microbial activity, are all impacted by aggregate stability (Liu et al., 2022; Tian et al., 2022). Furthermore, both intrinsic soil characteristics—such as particle composition, organic matter content, and clay mineralogy—and external factors—such as weathering, tillage methods, and erosion—have an impact on aggregate stability (Cao et al., 2016; Das et al., 2014;

https://doi.org/10.5194/egusphere-2026-1761
Preprint. Discussion started: 23 June 2026

Zhang et al., 2021). Therefore, improving soil aggregate stability is essential for reducing soil erodibility, improving soil health and sustaining agricultural productivity.

The application of biochar as a soil amendment is primarily attributed to its ability to boost organic carbon content and contribute to better soil functionality (Cooper et al., 2020; Ji et al., 2024; Lu et al., 2021; Okebalama and Marschner, 2023; Uchenna et al., 2023; Zhang et al., 2020). Numerous studies have demonstrated that biochar have successfully raised soil organic carbon levels and improved soil aggregate stability (Du et al., 2016; Huang et al., 2018; Ma et al., 2016; Sheng et al., 2023; Šimanský et al., 2018; Sun et al., 2021; Wang et al., 2017). However, Blair et al. (1995) concluded that anthropogenic management practices in agricultural systems primarily affect the reactive organic carbon fraction of soil organic carbon. Soil organic matter has been found to degrade slowly, making short-term changes in its content of limited practical significance. As an early and quick sign of ecosystem management techniques, soil active organic carbon, on the other hand, is less plentiful but more sensitive to environmental changes than soil organic matter (Coleman et al., 1983; Stevenson, 1994; Wander et al., 1994).

According to Haynes (2005) and Wei et al. (2014), soil active organic carbon represents the most dynamic fraction of soil organic carbon that has the greatest direct impact on plant nutrient supply; it is highly reactive, has a certain solubility in the soil, and is readily oxidized and mineralized by soil microorganisms. Light fraction organic carbon (LFOC), dissolved organic carbon (DOC), particulate

https://doi.org/10.5194/egusphere-2026-1761
Preprint. Discussion started: 23 June 2026

organic carbon (POC), and readily oxidized organic carbon (ROC) are the primary forms of soil active organic carbon (Stewart et al., 2009; Yang et al., 2017; Zhao et al., 2018). Despite making up a small fraction of soil organic carbon, soil active carbon has a direct role in soil biochemical transformation processes and can indicate slight variations in soil organic carbon before changes in total soil carbon (Coleman et al., 1983; Wander et al., 1994). Accordingly, variations in the amount of organic carbon's active fraction in agricultural soils significantly impact on the soil's nutrient cycling and overall quality (Liang et al., 2011; Magill and Aber, 2000).

Overall, increased soil active organic carbon enhances soil aggregate stability (Bronick and Lal, 2005). It has been demonstrated that soil active organic carbon fractions can affect the nutrient content and bioavailability of the soil and have a significant and positive correlation with the formation and stability of soil macroaggregates (Wang et al., 2018). Aggregate stability was shown to increase positively with organic carbon content, mainly in the light organic matter component (Yagüe et al., 2016). In comparison to soils treated with nitrogen, phosphorus, and potassium (NPK) in combination with green manure or NPK alone, Li et al. (2012) found that soils treated with NPK and animal manure had significantly higher levels of biologically active soil organic carbon and aggregate stability. Microaggregates and silt + clay fractions showed a significant negative association with the mean weight diameter and geometric mean diameter of soil aggregates, while DOC, macroaggregates, macroaggregates-C, and

https://doi.org/10.5194/egusphere-2026-1761
Preprint. Discussion started: 23 June 2026

microaggregates-C showed a significant positive correlation (Cao et al., 2024). In trials with simulated rainfall, soil aggregate stability rose when soil organic carbon and LFOC levels increased (Li et al., 2021). Although the role of active organic carbon in enhancing soil aggregate stability has been widely studied, the composition and characteristics of its various forms differ substantially, potentially leading to divergent effects on aggregate stability. Therefore, further research is needed to elucidate how different fractions of soil active organic carbon influence the formation and stabilization of soil aggregates.

The stability of soil aggregates in water is mostly due to soil internal forces (SIFs), which include electrostatic, hydration, and van der Waals attraction (Hu et al., 2015; Ma et al., 2021b). Theoretically, internal forces may reach hundreds of thousands of atmospheric pressures between two adjacent soil particles (Ding et al., 2019; Ma et al., 2022; Xu et al., 2015). The classical double layer theory states that the characteristics of the soil, including its specific surface area (SSA), surface charge density, and cation exchange capacity, as well as external environmental factors (moisture content, solution concentration, etc.), primarily determine the function of SIFs in mesoscale soils (Li et al., 2013; Quirk, 1994). The addition of organic matter modifies SIFs by altering the interfacial properties of soil particles. In a four-year field experiment, the use of weathered coal and biochar had a significant impact on the SSA and surface charge density of soil particles, as well as improving van der Waals attraction, decreasing net soil pressure, and decreasing aggregate fragmentation strength and splash erosion rate (Wang et al., 2024). Changes in the electrochemical

https://doi.org/10.5194/egusphere-2026-1761
Preprint. Discussion started: 23 June 2026

characteristics of the soil surface were mostly caused by an increase in the amount of soil organic matter after vegetation restoration (Liu et al., 2020). Nevertheless, few research have examined how various active organic carbon fractions affect SIFs and aggregate stability by altering the surface properties of the soil particles when biochar is applied.

In this study, maize straw and wheat straw biochars were applied at different rates in a field simulation experiment to systematically evaluate their effects on soil internal forces. Specifically, we aimed to (i) quantify the changes in SIFs under different biochar types and application rates, (ii) identify the active organic carbon fractions that most strongly regulate soil interfacial electrochemical properties and thereby influence SIFs, and (iii) elucidate the mechanisms and time effects by which biochar-mediated modifications of SIFs contribute to soil aggregate formation and stabilization. This work provides new mechanistic insights into biochar–soil interactions from the perspective of soil internal forces and offers a scientific basis for targeted soil structural improvement and sustainable agricultural management.

2. Materials and methods

2.1 Study area

This study was conducted in the Yangling Demonstration Zone, Shaanxi Province, China (108°08′47″E，34°27′21″N). The region has a temperate continental monsoon semi-humid climate, with an average of 2167 hours of sunlight per year, temperatures between 11 and 13 ℃, and 500 to 700 mm of rainfall. According to the FAO soil classification, the soil under study was Lou soil, which is categorized as

https://doi.org/10.5194/egusphere-2026-1761
Preprint. Discussion started: 23 June 2026

calcareous Cambisol. The basic physicochemical properties of the soil are shown in Table 1.

2.2 Experimental design

The biochar made from wheat and maize straw that was utilized in this investigation was acquired from Zhengzhou Jinbang Environmental Protection Technology Co. An elemental analyzer (Elementar Vario EL III, Germany) was used to determine the elemental composition of the biochar samples. A fully automated specific surface and porosity analyzer (Micromeritics ASAP 2460, USA) was used to measure the SSA of biochar. A Mettler pH meter with a solid-liquid ratio of 1: 20 was used to measure the pH. The amount of ash was measured by placing the biochar in a crucible and burning it for two hours at 800 ℃. Table 2 displays the fundamental physical and chemical characteristics of biochar.

In mid-December 2021, biochar was added to the top layer of soil (0–20 cm) and tilled lightly until it was incorporated into the soil. In a control treatment (CK), no biochar was used. Two varieties of biochar, manufactured from maize and wheat straw, were treated at five different dose levels: 1%, 3%, 5%, and 10% by mass (designated M1, M3, M5, and M10 for maize straw biochar; W1, W3, W5, and W10 for wheat straw biochar). There were 27 plots in all, each measuring 1.5 m by 1.5 m, and a completely randomized design with three replications was employed (Figure 1). At the end of the 180-day and 365-day experimental periods, five soil auger samples were collected from the 0–20 cm layer of each plot and combined to form a composite soil sample. The samples were then allowed to dry naturally and were ready for use

https://doi.org/10.5194/egusphere-2026-1761
Preprint. Discussion started: 23 June 2026

after being cleared of stones, plant roots, and other contaminants. Before determining the soil properties, the unbound biochar particles in the soil samples were floated off in distilled water.

2.3 Determination of soil active organic carbon and electrochemical properties

A carbon and nitrogen analyzer (Multi N/C 3000, Jena, Germany) was used to measure DOC (Qiu et al., 2023). By using potassium permanganate for oxidation, ROC was determined (Zhang et al., 2022). Sulfuric acid-potassium dichromate oxidation with external heating and sodium iodide heavy liquid separation were used to calculate LFOC (Janzen et al., 1992). Sulfuric acid-potassium dichromate oxidation using an external heating technique and sodium hexametaphosphate dispersion were used to determine POC (Ma et al., 2021a).

The combined method of surface property determination provided by Li et al. (2011) was used to measure the soil surface charge number (SCN), surface charge density (σ_0), and SSA. In short, soil samples were subjected to exchange equilibrium testing using a combination of NaOH and $Ca(OH)_2$ after being pre-saturated with H^+. After measuring the amounts of Na^+ and Ca^{2+} in the supernatant, the double-layer theory was used to compute the cation exchange capacity, SSA, and σ_0; the detailed procedures can be found in our previous work (Hu et al., 2021).

2.4 Quantification of soil internal forces

At the mesoscopic level, the primary SIF interactions among soil particles are van der Waals attractive pressure (P_{vdw}), surface hydration repulsive pressure (P_h), and electrostatic repulsive pressure (P_E). The net inter-particle force (P_{net}) is the

https://doi.org/10.5194/egusphere-2026-1761
Preprint. Discussion started: 23 June 2026

combined force of the three, which can be calculated from the soil surface property parameter to obtain the SIFs (Li and Xu, 2008; Liu et al., 2021).

2.5 Soil aggregate stability evaluation

In this experiment, soils were prepared as Na^+-saturated samples to quantitatively characterize the intrinsic link between SIFs and aggregate stability. Soil aggregate breaking strength (SABS) was used to evaluate the aggregate stability (Xu et al., 2015). It was defined as the proportion of mass released as small particles (less than 5 and less than 10 μm) when macroaggregates broke down. As the percentage mass release increases, soil aggregate stability decreases. The following was the preparation procedure: A 5 L beaker containing 2 kg of air-dried soil was filled with 5 L of NaCl electrolyte solution at a concentration of 0.5 mol L^{-1}. The sample was centrifuged and the supernatant was disposed of after 24 hours of stirring and equilibration. Following three repetitions of the aforementioned procedure, the extra Na^+ was removed using distilled water and dried through a 1–5 mm sieve. Different concentrations of NaCl solutions (10^{-5}, 10^{-3}, 10^{-2}, 10^{-1}, 1 mol L^{-1}) were used in the experiment to simulate soil electrolyte solutions. The time required for < 10 μm and < 5 μm soil particles to fall at a specific distance was first calculated according to Stokes formula, respectively. About 450 ml of a NaCl solution with concentrations of 1, 10^{-1}, 10^{-2}, 10^{-3}, and 10^{-5} mol L^{-1} was put into a 500 ml measuring cylinder. Weigh 15 g of Na^+-saturated aggregates and transfer them into a measuring cylinder. Add the same solution to bring the total volume to 500 mL, then seal the cylinder. Allow it to stand for 1 minute. Afterward, hold the cylinder

https://doi.org/10.5194/egusphere-2026-1761
Preprint. Discussion started: 23 June 2026

horizontally in your hand and rotate it slowly, inverting it once and allowing it to stand for approximately 30 seconds. Repeat this process four times. Finally, place the cylinder on the tabletop, record the start time, and calculate the end time. A U-shaped tube was used to aspirate the suspension at the conclusion of the allotted period, and it was then moved into an aluminum box. The sample was then weighed after drying at 105 ℃, following the method of Hu et al. (2015).

2.6 Statistical analysis

Microsoft Excel was used to arrange and compute the data, while SPSS Statistics 26 was used to conduct the statistical analysis. Statistical significance was determined using Duncan's test ($P < 0.05$). The relationship between soil surface electrochemical characteristics and soil active carbon fractions was assessed using the Pearson's coefficient test. Soil carbon fractions and electrochemical properties were analyzed redundantly using Canoco 5.0. Origin 2023 software was applied for data plotting.

3. Results

3.1 Effect of biochar addition on soil active organic carbon fractions

After applying maize straw biochar and wheat straw biochar after 180 days, the overall amount of soil active organic carbon rose as the amount of biochar increased (Figure 2). Both biochar treatments significantly increased soil LFOC concentrations ($P < 0.05$), although slight, non-significant decreases were observed in the M5 and W5 treatments compared to M3 and W3. The M10 and W10 treatments showed the highest increase, 147.9 and 127.0 times compared to CK, respectively. The LFOC under each treatment for the two kinds of straw biochar was only substantially

https://doi.org/10.5194/egusphere-2026-1761
Preprint. Discussion started: 23 June 2026

different at the 10% addition rate; at the 3% and 5% biochar application rates, the difference was not significant (Figure 2a). Both biochar treatments significantly enhanced soil POC content ($P < 0.05$). In terms of magnitude, M10 and W10 exhibited the largest increases, with POC contents 84.2 and 78.4 times higher than that of the CK, respectively. With the exception of the 5% application rate (Figure 2b), no appreciable variations in the soil POC concentration were noted in relation to the impacts of the two straw biochar treatments at the same application rate. The M10 and W10 treatments increased DOC by 18.6 and 18.1 times, respectively, compared to CK. At the same application rate, there were no discernible variations in DOC between the two biochars (Figure 2c). The M10 and W10 treatments increased ROC by 5.1 and 5.3 times, respectively, compared to CK. At the same application rate, there were no discernible variations in ROC between the two biochars (Figure 2d). The contents of different carbon fractions under each treatment decreased with the extension of incubation time, and the data for soil active carbon fractions at 365 days are provided in Supplementary Figure S1.

3.2 Effect of biochar addition on soil surface electrochemical properties

Table 3 shows that as the amount of biochar rose from 0% to 10%, SCN increased considerably ($P < 0.05$). Compared with CK, SCN increased by 23.3%, 33.3%, 39.8%, and 42.7% under each treatment of maize straw biochar, and 27.1%, 33.3%, 39.4%, and 46.4% under the wheat straw biochar treatment, respectively. The difference between the two biochars at the same addition level was not significant. The soil SSA increased significantly ($P < 0.05$) with increasing biochar application

https://doi.org/10.5194/egusphere-2026-1761
Preprint. Discussion started: 23 June 2026

rates; the M1 treatment and CK did not differ significantly, and at 1%, 3%, and 5% application rates, the differences between the treatments were not significant, and M10 and W10 increased by 91.06% and 91.53%, respectively, in comparison to the CK treatment. Surface charge density σ_0 showed no significant change at lower application rates (1%, 3%, 5%) compared to CK. However, σ_0 tended to decline as biochar application rate increased. After 365 days of incubation with biochar, the trends of soil electrochemical parameters were consistent with those observed at 180 days, and the values of these parameters were slightly higher than those at 180 days. The data for soil surface electrochemical properties at 365 days are provided in Supplementary Table S1.

3.3 Relationship between soil electrochemical properties and active carbon fractions

After 180 days of biochar application, the correlation between soil electrochemical properties and active organic carbon fractions is presented in Figure 3a. SCN exhibited a strong positive association with LFOC and POC ($P < 0.05$) and a highly significant positive correlation with DOC and ROC ($P < 0.01$). SSA and DOC ($P < 0.01$), LFOC, POC, and ROC ($P < 0.001$) all showed a substantial positive connection. In contrast, σ_0 was strongly negatively correlated with LFOC, POC, and ROC ($P < 0.001$), and with DOC ($P < 0.01$). The results at 365 days (Fig. 3b) showed that SCN and SSA were significantly and positively correlated with LFOC, POC, DOC, and ROC ($P < 0.001$). In contrast, σ_0 was negatively correlated with LFOC, POC, and ROC ($P < 0.05$), and showed a highly significant negative correlation with

https://doi.org/10.5194/egusphere-2026-1761
Preprint. Discussion started: 23 June 2026

DOC ($P < 0.001$).

Figure 4 displays the results of redundancy analysis. The results showed that after 180 days of biochar addition, ROC explained 63.6% of the variation in soil electrochemical properties, whereas after 365 days, POC accounted for 66.1% of the variation (Table 4). Therefore, ROC and POC are the primary factors influencing the electrochemical properties of the soil surface. The acute angle formed between the SCN, SSA, and soil active carbon component arrows indicates a strong positive correlation between them (the smaller the acute angle, the stronger the relationship), consistent with the results in Figure 3.

3.4 Effect of biochar addition on soil internal forces

3.4.1 Electrostatic repulsive pressure between soil particles

The electrostatic repulsive pressure at various electrolyte concentrations at a distance of 2 nm between soil particles is depicted in Figure 5. The findings demonstrated that as the amount of maize straw and wheat straw biochar applied rose from 1% to 10%, the electrostatic repulsive pressure gradually reduced at the same electrolyte concentration. At a constant biochar application rate, electrostatic repulsive pressure increased sharply under all treatments as the electrolyte concentration decreased progressively from 1 mol L^{-1} to 10^{-2} mol L^{-1}. However, when the electrolyte concentration is further decreased below 10^{-2} mol L^{-1}, the rate of growth of electrostatic repulsive pressure slows down and stabilizes. After 365 days of incubation, the trends in electrostatic repulsive pressure for each treatment were consistent with those at 180 days, and increased compared to the soil after 180 days of

https://doi.org/10.5194/egusphere-2026-1761
Preprint. Discussion started: 23 June 2026

incubation.

3.4.2 Van der Waals attractive pressure and surface hydration repulsive pressure

Table 5 shows that all of the Hamaker constant values were higher than CK and rose as the amount of biochar applied increased. The strength of the van der Waals attractive pressure between soil particles is directly determined by the Hamaker constant, a crucial element in the computation of this pressure. The amount and distribution of the van der Waals attractive pressure and surface hydration repulsive pressure between particles with biochar addition after 180 and 365 days (as seen in Figure 6) may be determined using the formula, in conjunction with the acquired Hamaker constant. The van der Waals attractive pressure (absolute value) and the surface hydration repulsive pressure both sharply decline with increasing soil particle distance. When the spacing between soil particles was smaller than 1.3 nm, the surface hydration repulsive pressure was substantially larger in all treatments than the van der Waals attractive pressure. For instance, under various treatments, the interparticle van der Waals attractive pressure (in absolute value) is less than 100 atm and the interparticle surface hydration repulsive pressure is around 591 atm when the interparticle distance is 0.7 nm. The van der Waals attractive pressure (absolute values) is all below 200 atm, but the surface hydration repulsive pressure is around 1051 atm at an interparticle distance of 0.6 nm. This suggests that the difference between the two rises quickly as the distance decreases. Van der Waals attractive pressure (absolute value) rose with increasing application rate in both biochar treatments. After 365 days of incubation, the trends in the Hamaker constant and van der Waals

https://doi.org/10.5194/egusphere-2026-1761
Preprint. Discussion started: 23 June 2026

attraction (in absolute value) for each treatment were consistent with those at 180 days, and increased compared to the soil after 180 days of incubation.

3.4.3 Net pressure between soil particles

Figure 7 shows the net pressure of soil particles at 2 nm for different electrolyte concentrations under biochar addition after 180 and 365 days. Under both biochar types, net pressure increased as electrolyte concentration decreased. From 1 mol L^{-1} to 10^{-2} mol L^{-1}, net pressure rose markedly; below 10^{-2} mol L^{-1}, the rate of increase plateaued. At the same electrolyte concentration, net pressure decreased as biochar application increased. After 365 days of incubation, the trends in the net interparticle force were consistent with those at 180 days, and decreased compared to the soil after 180 days of incubation.

3.5 Effect of biochar addition on soil aggregate stability

Figure 8 shows SABS (< 5 μm, < 10 μm) at different electrolyte concentrations under biochar addition after 180 days. As the electrolyte concentration increased, the SABS decreased. The change in SABS was relatively smooth when the electrolyte concentration was less than 10^{-2} mol L^{-1}, but it significantly decreased for all treatments when the electrolyte concentration went from 10^{-2} to 1 mol L^{-1}. A concentration of 10^{-2} mol L^{-1} represents the critical threshold for aggregate disintegration. SABS dropped as biochar application increased under the same electrolyte concentration, suggesting that biochar application improved aggregate stability. After 365 days of incubation, the trends in aggregate breaking strength for each treatment were consistent with those at 180 days, and the values decreased

https://doi.org/10.5194/egusphere-2026-1761
Preprint. Discussion started: 23 June 2026

compared to the soil after 180 days of incubation. The data for soil aggregate breaking strength at 365 days are provided in Supplementary Figure S2.

3.6 Relationship between soil internal forces and aggregate stability

Figure 9 depicts the relationship between the net pressure at a 2 nm distance between soil particles and SABS under biochar addition after 180 and 365 days. The figure reveals a significant positive correlation between SABS and net pressure across all treatments, with SABS exhibiting an exponential increase in response to rising net pressure.

4. Discussion

4.1 Response of soil active carbon fraction and electrochemical properties to biochar application

The application of biochar enhanced soil active carbon fractions and had a considerable impact on soil organic carbon (Han et al., 2020; Li et al., 2024; Lu et al., 2021; Yang et al., 2017; Zhao et al., 2018). According to our findings, the soil active carbon percentage rose when both types of biochar were added (Figure 2 and Figure S1). The reason can be explained: the biochar itself contains more carbon, especially more resistant humic acid and condensed aromatic carbon structures. Secondly, biochar possesses a large surface area, which may facilitate the accumulation of specific organic carbon fractions in the soil by adsorbing them onto its surface. Biochar has a highly porous structure that also protects some organic carbon components from microbial degradation (Feng et al., 2021; He et al., 2023). In a field experiment, Qiu et al. (2023) applied biochar to 0%, 1%, 2%, and 4% of the dry

https://doi.org/10.5194/egusphere-2026-1761
Preprint. Discussion started: 23 June 2026

weight of topsoil. After 8 and 12 months, they observed a positive correlation between the amount of particulate organic carbon and the amount of biochar applied, as well as significant increases in organic carbon, particulate organic carbon, and DOC content. In comparison to the control, soil organic carbon, ROC, and POC levels rose by 7.09–38.08%, 1.62–39.80%, and 9.52–62.30%, respectively, when Jiang et al. (2022) applied 0, 5, 15, 20, and 40 t ha^{-1} of biochar to the soil. As a result, soil active carbon fractions were significantly impacted by biochar additions.

With the extension of incubation time from 180 days to 365 days, the content of soil active carbon fractions decreased, which may be attributed to several factors (Stewart et al., 2009; Yang et al., 2017; Zhao et al., 2018). Firstly, as the incubation period increased, organic carbon in the soil was gradually degraded and mineralized by microorganisms, leading to a decrease in the content of ROC and DOC. Secondly, the long-term application of biochar may have transformed some organic carbon into more stable forms, which are less susceptible to microbial decomposition, resulting in a decline in the active organic carbon fractions. Additionally, changes in the soil environment, such as fluctuations in moisture, temperature, and pH, may have affected the availability and turnover rate of organic carbon, further contributing to the reduction in active organic carbon content.

Both biochar applications considerably raised the SSA and SCN of soil particles in this investigation (Table 2 and Table S1). According to Liang et al. (2006), this phenomenon is caused by the numerous negative charges that are carried on the surface of biochar. These charges come from the oxygen-containing functional groups,

https://doi.org/10.5194/egusphere-2026-1761
Preprint. Discussion started: 23 June 2026

like -COOH, -OH, etc., that are widely distributed on the surface of biochar and which effectively improve the cation exchange of the soil. The high SSA of biochar itself directly contributes to an increase in soil SSA, improves cation adsorption, and thus enhances exchange capacity (Lone et al., 2015). Consistent with Hu et al. (2021), our findings show that increasing the biochar application rate enhances soil SSA and SCN (Table 2 and Table S1). However, the increase in soil organic carbon (particularly the active carbon component) brought about by the addition of biochar may have contributed to the rise in SSA and SCN. The study's findings demonstrated that adding two different kinds of biochar raised the amount of active carbon in the soil and that there was a significant relationship between soil active carbon and soil electrochemical characteristics, with ROC and POC being the primary determinant of the soil surface's electrochemical characteristics (Table 4; Figures 3–4). According to Meyer et al. (1994) and Pennell et al. (1995), soil organic matter, particularly humic acid, has a cation exchange capacity of up to 100–700 cmol(c) kg^{-1} and an SSA of up to 500–800 m^2 g^{-1}. Vertisol soil SSA (about 35.3%) and SCN (approximately 29.3%) were shown to decrease with the removal of soil organic matter (Yu et al., 2020). Compared with more stable organic carbon pools, ROC represents the relatively amorphous, chemically reactive fraction that is enriched in oxygen-containing functional groups (e.g. –COOH, –OH, –C=O) and is preferentially adsorbed onto or co-precipitated with mineral surfaces. Such functional groups provide abundant negatively charged sites and enhance the development of the diffuse double layer, thereby increasing soil SSA, SCN and surface charge density and modifying the

https://doi.org/10.5194/egusphere-2026-1761
Preprint. Discussion started: 23 June 2026

445 balance between electrostatic repulsion and van der Waals attraction at the particle–
446 water interface (He et al., 2021). In contrast, POC is typically found in smaller soil
447 particles and influences the electrochemical properties of the soil surface through
448 physical adsorption. The role of POC primarily involves its interaction and stability
449 with minerals, which increases the charge and physical surface characteristics of the
450 soil, further regulating the soil's electrochemical behavior. ROC and POC jointly
451 influence the electrochemical properties of the soil, with ROC being more sensitive to
452 changes in soil electrochemical properties in the short term, while POC affects the
453 soil's electrochemical reactions over a longer period through stable mineral-organic
454 carbon complexes. These organic carbon fractions have been repeatedly identified as
455 a sensitive indicator of short-term management effects and is closely linked to key
456 fertility parameters, including effective CEC and other electrochemical properties
457 (Culman et al., 2012). Therefore, soil active organic carbon (especially ROC and POC)
458 is closely related to the electrochemical properties of the soil surface.

459 **4.2 Response of soil internal forces to biochar application**

460 Soil particles in close proximity experience mutual repulsion due to like charges,
461 generating electrostatic repulsive pressure. Because soil texture, organic matter
462 content, and mineral composition all affect the particles' surface charge, variations in
463 these characteristics will result in variations in electrostatic repulsive pressure (Hu et
464 al., 2015; Liu et al., 2021). At the same electrolyte concentration, soil electrostatic
465 repulsive pressure decreased under both biochar treatments as biochar application
466 increased from 1% to 10% (Figure 5). This phenomenon is caused by the substantial

https://doi.org/10.5194/egusphere-2026-1761
Preprint. Discussion started: 23 June 2026

alterations in the electrochemical characteristics of the soil surface, which are shown by the increase in SCN and SSA, the decrease in the intensity of the surface electric field and charge density, and the effective control of electrostatic repulsive pressure. Both forms of biochar reduced electrostatic repulsive pressure similarly, which was essentially in line with the trend of soil surface electrochemical parameters under varying rates of biochar application, which is in line with Wang et al. (2024) findings.

Biochar application also significantly increased van der Waals attractive pressure between soil particles, particularly at higher application rates (Figure 6). Van der Waals pressure is directly related to the Hamaker constant, which itself depends on the properties of the materials and the intervening medium (Bergström, 1997; Hu et al., 2021; Yu et al., 2020). The observed increases in Hamaker constants (Table 4) suggest that biochar incorporation introduced more organic complexes into the soil (Resurreccion et al., 2011). Additionally, our results revealed that net interparticle pressure decreased as biochar application increased (Figure 7), consistent with the findings of Yu et al. (2017). These results suggest that the influence of biochar on net pressure is primarily through increased van der Waals attraction and reduced electrostatic repulsion.

4.3 Response of soil aggregate stability to biochar application

In this study, SABS values decreased with increasing biochar application (Figure 8 and Figure S2), indicating improved aggregate stability. This aligns with previous findings that biochar enhances soil aggregation (Fu et al., 2021; He et al., 2020; Luo et al., 2020; Sun et al., 2021; Wang et al., 2022). The observed decline in net pressure

https://doi.org/10.5194/egusphere-2026-1761
Preprint. Discussion started: 23 June 2026

with increasing biochar (Figure 7) supports this conclusion, as lower internal forces correspond to greater structural stability. This is consistent with prior reports by Yu et al. (2020) and Hu et al. (2021), who also found that biochar reduces internal particle forces and enhances aggregate stability.

We also observed that SABS increased with decreasing electrolyte concentration and then plateaued, with a threshold near 10^{-2} mol L^{-1}, indicating a critical transition in aggregate disintegration. This turning point corresponded to a similar trend in net interparticle pressure, reinforcing the connection between soil internal forces and aggregate stability. Regression analysis confirmed a significant positive correlation between SABS and net pressure (Figure 9), highlighting the central role of interparticle forces in determining aggregate stability.

The effectiveness of biochar in improving soil aggregation depends on environmental conditions, soil type, and feedstock characteristics (Du et al., 2016; Fungo et al., 2017; Jien and Wang, 2013; Pituello et al., 2018; Yang and Lu, 2021; Zhang et al., 2015). Overall, there were no significant differences in SIF distribution and aggregate stability between the two biochar treatments in this study. This may be attributed to the fact that the basic properties of the two types of straw biochar are relatively similar (Table 2). Additionally, there were no significant changes in the active carbon components and surface electrochemical properties of the soil after the two types of biochar were added. In addition, our study found that the improvement in soil aggregate stability was greater at 365 days compared to 180 days following the application of both types of biochar. This is because, compared to 180 days, biochar

https://doi.org/10.5194/egusphere-2026-1761
Preprint. Discussion started: 23 June 2026

addition at 365 days increased both soil charge density and the Hamaker constant, which in turn enhanced both the electrostatic repulsive force and molecular attraction at the mesoscale between soil particles. However, the increase in molecular attraction was much greater than that of electrostatic repulsion, resulting in a lower net force. Therefore, soil aggregate stability was stronger after 365 days of biochar addition.

Although this study focused on short-term (365-day) effects, biochar is known for its long-term stability in soil environments. Previous research has shown that biochar can enhance soil aggregation, nutrient retention, and carbon sequestration for years to decades (Jiang et al., 2022; Sun et al., 2021). However, these long-term benefits may be affected by aging processes, environmental variability, and management practices. Future long-term field experiments are needed to better understand the persistence and dynamics of biochar effects in diverse agroecosystems.

5. Conclusions

After 180 and 365 days of maize straw biochar and wheat straw biochar addition, the contents of soil active carbon fractions increased with higher biochar application rates. Soil active carbon fractions were closely related to soil electrochemical properties, with ROC and POC being the primary influencing factors. The application of biochar markedly modified the SSA and SCN of soil particles, thereby increasing van der Waals attractive forces, reducing net repulsive pressure, and ultimately enhancing aggregate stability. These beneficial effects were further amplified as the application rate increased. As the electrolyte concentration decreased, the SABS first increased and then tended to level off, and 10^{-2} mol L^{-1} was the turning point for the

https://doi.org/10.5194/egusphere-2026-1761
Preprint. Discussion started: 23 June 2026

change. Although this study utilized Na^+-saturated soil samples, which do not fully reflect natural soil conditions, the findings quantitatively assessed the intensity and distribution of soil internal forces (SIFs) and elucidated the mechanistic pathway by which biochar-induced increases in ROC and POC, along with associated changes in soil surface electrochemistry, enhance aggregate stability. Collectively, these findings offer a theoretical basis for the targeted use of biochar to manipulate soil internal forces, strengthen aggregate structure, and mitigate soil erosion in agricultural systems.

Code and data availability

No custom code was used in this study. The experimental data that support the findings of this study are available from the corresponding author upon reasonable request.

Acknowledgements

This work was supported by the National Natural Science Foundation of China (42277311 and 42361144707), the Open Found from the State Key Laboratory of Soil and Water Conservation and Desertification Control (F2010121002-202419), Natural Science Foundation of Shaanxi Province (2023-JC-YB-263) and the Natural Science Foundation of Chongqing, China (CSTB2024NSCQ-LZX0020).

References

https://doi.org/10.5194/egusphere-2026-1761
Preprint. Discussion started: 23 June 2026

555 An, S.S., Mentler, A., Mayer, H., Blum, W.E.H., 2010. Soil aggregation, aggregate
556 stability, organic carbon and nitrogen in different soil aggregate fractions under
557 forest and shrub vegetation on the Loess Plateau, China. Catena 81, 226-233.
558 http://doi.org/10.1016/j.catena.2010.04.002.
559 Batista, A.M., Nunes, M.R., Pessoa, T.N., Libardi, P.L., 2023. Seasonal variation of
560 the rhizosphere soil aggregation in an Oxisol. Soil Tillage Res. 231.
561 http://doi.org/10.1016/j.still.2023.105741.
562 Bergström, L., 1997. Hamaker constants of inorganic materials. Adv. Colloid
563 Interface Sci. 70, 125-169. http://doi.org/10.1016/s0001-8686(97)00003-1.
564 Blair, G.J., Lefroy, R.D.B., Lisle, L., 1995. Soil carbon fractions based on their degree
565 of oxidation, and the development of a carbon management index for agricultural
566 systems. Aust. J. Agric. Res. 46. http://doi.org/10.1071/ar9951459.
567 Bronick, C.J., Lal, R., 2005. Soil structure and management: a review. Geoderma 124,
568 3-22. http://doi.org/10.1016/j.geoderma.2004.03.005.
569 Cao, X., Xu, Y., Wang, F., Zhang, Z., Xu, X., 2024. Changes of soil organic carbon
570 and aggregate stability along elevation gradient in Cunninghamia lanceolata
571 plantations. Sci Rep 14, 31778. http://doi.org/10.1038/s41598-024-81847-4.
572 Cao, Z.Y., Wang, Y., Li, J., Zhang, J.J., He, N.P., 2016. Soil organic carbon contents,
573 aggregate stability, and humic acid composition in different alpine grasslands in
574 Qinghai-Tibet Plateau. J Mt. Sci. 13, 2015-2027.
575 http://doi.org/10.1007/s11629-015-3744-y.
576 Coleman, D.C., Reid, C.P.P., Cole, C.V., 1983. Biological Strategies of Nutrient

https://doi.org/10.5194/egusphere-2026-1761
Preprint. Discussion started: 23 June 2026

Cycling in Soil Systems, Adv. Ecol. Res., pp. 1-55.

Cooper, J., Greenberg, I., Ludwig, B., Hippich, L., Fischer, D., Glaser, B., Kaiser, M., 2020. Effect of biochar and compost on soil properties and organic matter in aggregate size fractions under field conditions. Agric. Ecosyst. Environ. 295. http://doi.org/10.1016/j.agee.2020.106882.

Culman, S.W., Snapp, S.S., Freeman, M.A., Schipanski, M.E., Beniston, J., Lal, R., Drinkwater, L.E., Franzluebbers, A.J., Glover, J.D., Grandy, A.S., Lee, J., Six, J., Maul, J.E., Mirksy, S.B., Spargo, J.T., Wander, M.M., 2012. Permanganate Oxidizable Carbon Reflects a Processed Soil Fraction that is Sensitive to Management. Soil Sci. Soc. Am. J. 76, 494-504. http://doi.org/10.2136/sssaj2011.0286.

Das, B., Chakraborty, D., Singh, V.K., Aggarwal, P., Singh, R., Dwivedi, B.S., Mishra, R.P., 2014. Effect of integrated nutrient management practice on soil aggregate properties, its stability and aggregate-associated carbon content in an intensive rice–wheat system. Soil Tillage Res. 136, 9-18. http://doi.org/10.1016/j.still.2013.09.009.

Ding, W., Liu, X., Hu, F., Zhu, H., Luo, Y., Li, S., Li, H., 2019. How the particle interaction forces determine soil water infiltration: Specific ion effects. J. Hydrol. 568, 492-500. http://doi.org/10.1016/j.jhydrol.2018.11.017.

Du, Z.-L., Zhao, J.-K., Wang, Y.-D., Zhang, Q.-Z., 2016. Biochar addition drives soil aggregation and carbon sequestration in aggregate fractions from an intensive agricultural system. J. Soils Sediments 17, 581-589.

https://doi.org/10.5194/egusphere-2026-1761
Preprint. Discussion started: 23 June 2026

599 http://doi.org/10.1007/s11368-015-1349-2.

600 Feng, Z., Fan, Z., Song, H., Li, K., Lu, H., Liu, Y., Cheng, F., 2021. Biochar induced
601 changes of soil dissolved organic matter: The release and adsorption of dissolved
602 organic matter by biochar and soil. Sci. Total Environ. 783, 147091.
603 http://doi.org/10.1016/j.scitotenv.2021.147091.

604 Fu, G.Q., Qiu, X.N., Xu, X.Y., Zhang, W., Zang, F., Zhao, C.Y., 2021. The role of
605 biochar particle size and application rate in promoting the hydraulic and physical
606 properties of sandy desert soil. Catena 207.
607 http://doi.org/10.1016/j.catena.2021.105607.

608 Fungo, B., Lehmann, J., Kalbitz, K., Thiongo, M., Okeyo, I., Tenywa, M., Neufeldt,
609 H., 2017. Aggregate size distribution in a biochar-amended tropical Ultisol under
610 conventional hand-hoe tillage. Soil Tillage Res. 165, 190-197.
611 http://doi.org/10.1016/j.still.2016.08.012.

612 Han, L., Sun, K., Yang, Y., Xia, X., Li, F., Yang, Z., Xing, B., 2020. Biochar's stability
613 and effect on the content, composition and turnover of soil organic carbon.
614 Geoderma 364. http://doi.org/10.1016/j.geoderma.2020.114184.

615 Haynes, R.J., 2005. Labile organic matter fractions as central components of the
616 quality of agricultural soils: An overview, Adv. Agron., pp. 221-268.

617 He, L.L., Zhao, J., Yang, S.M., Zhou, H., Wang, S.Q., Zhao, X., Xing, G.X., 2020.
618 Successive biochar amendment improves soil productivity and aggregate
619 microstructure of a red soil in a five-year wheat-millet rotation pot trial.
620 Geoderma 376. http://doi.org/10.1016/j.geoderma.2020.114570.

https://doi.org/10.5194/egusphere-2026-1761
Preprint. Discussion started: 23 June 2026

621 He, M.R., Jiang, Y., Han, Y.H., Zhu, W.H., Meng, D., Li, C.L., Cai, H.G., Zhang, J.J.,
622 2023. Rice Straw Biochar is More Beneficial to Soil Organic Carbon
623 Accumulation and Stabilization than Rice Straw and Rice Straw Ash. J. Soil Sci.
624 Plant Nutr. 23, 3023-3033. http://doi.org/10.1007/s42729-023-01256-w.
625 He, Y., Yang, M., Huang, R., Wang, Y., Ali, W., 2021. Soil organic matter and clay
626 zeta potential influence aggregation of a clayey red soil (Ultisol) under long-term
627 fertilization. Sci Rep 11, 20498. http://doi.org/10.1038/s41598-021-99769-w.
628 Hu, F., Xu, C., Li, H., Li, S., Yu, Z., Li, Y., He, X., 2015. Particles interaction forces
629 and their effects on soil aggregates breakdown. Soil Tillage Res. 147, 1-9.
630 http://doi.org/10.1016/j.still.2014.11.006.
631 Hu, F., Xu, C., Ma, R., Tu, K., Yang, J., Zhao, S., Yang, M., Zhang, F., 2021. Biochar
632 application driven change in soil internal forces improves aggregate stability:
633 Based on a two-year field study. Geoderma 403.
634 http://doi.org/10.1016/j.geoderma.2021.115276.
635 Huang, R., Tian, D., Liu, J., Lu, S., He, X.H., Gao, M., 2018. Responses of soil
636 carbon pool and soil aggregates associated organic carbon to straw and
637 straw-derived biochar addition in a dryland cropping mesocosm system. Agric.
638 Ecosyst. Environ. 265, 576-586. http://doi.org/10.1016/j.agee.2018.07.013.
639 Janzen, H.H., Campbell, C.A., Brandt, S.A., Lafond, G.P., Townley-Smith, L., 1992.
640 Light-Fraction Organic Matter in Soils from Long-Term Crop Rotations. Soil Sci.
641 Soc. Am. J. 56, 1799-1806.
642 http://doi.org/10.2136/sssaj1992.03615995005600060025x.

https://doi.org/10.5194/egusphere-2026-1761
Preprint. Discussion started: 23 June 2026

643 Ji, D.C., Ge, L.W., Van Zwieten, L., An, T.T., Li, S.Y., Kuzyakov, Y., Ding, F., Wang,
644 J.K., 2024. Contrasting effects of maize straw and its biochar on aggregation and
645 soil organic matter stabilization. Plant Soil 495, 221-233.
646 http://doi.org/10.1007/s11104-023-06313-y.
647 Jiang, M.H., Li, C.B., Gao, W.C., Cai, K., Tang, Y., Cheng, J.Z., 2022. Comparison of
648 long-term effects of biochar application on soil organic carbon and its fractions
649 in two ecological sites in karst regions. Geoderma Reg. 28.
650 http://doi.org/10.1016/j.geodrs.2021.e00477.
651 Jien, S.H., Wang, C.S., 2013. Effects of biochar on soil properties and erosion
652 potential in a highly weathered soil. Catena 110, 225-233.
653 http://doi.org/10.1016/j.catena.2013.06.021.
654 Li, C.L., Xu, J.B., He, Y.Q., Liu, Y.L., Fan, J.B., 2012. Dynamic Relationship
655 Between Biologically Active Soil Organic Carbon and Aggregate Stability in
656 Long-Term Organically Fertilized Soils. Pedosphere 22, 616-622.
657 http://doi.org/10.1016/S1002-0160(12)60046-0.
658 Li, H., Hou, J., Liu, X.M., Li, R., Zhu, H.L., Wu, L.S., 2011. Combined
659 Determination of Specific Surface Area and Surface Charge Properties of
660 Charged Particles from a Single Experiment. Soil Sci. Soc. Am. J. 75, 2128-2135.
661 http://doi.org/10.2136/sssaj2010.0301.
662 Li, H.R., Liu, G., Gu, J., Chen, H., Shi, H.Q., Abd Elbasit, M.A.M., Hu, F.N., 2021.
663 Response of soil aggregate disintegration to the different content of organic
664 carbon and its fractions during splash erosion. Hydrol. Process. 35.

https://doi.org/10.5194/egusphere-2026-1761
Preprint. Discussion started: 23 June 2026

http://doi.org/10.1002/hyp.14060.

Li, Q., Zhang, J., Ye, J., Liu, Y., Lin, Y., Yi, Z., Wang, Y., 2024. Biochar affects organic carbon composition and stability in highly acidic tea plantation soil. J. Environ. Manage. 370, 122803. http://doi.org/10.1016/j.jenvman.2024.122803.

Li, S.-z., Xu, R.-k., 2008. Electrical double layers' interaction between oppositely charged particles as related to surface charge density and ionic strength. Colloid Surf. A-Physicochem. Eng. Asp. 326, 157-161. http://doi.org/10.1016/j.colsurfa.2008.05.023.

Li, S., Li, H., Xu, C.Y., Huang, X.R., Xie, D.T., Ni, J.P., 2013. Particle Interaction Forces Induce Soil Particle Transport during Rainfall. Soil Sci. Soc. Am. J. 77, 1563-1571. http://doi.org/10.2136/sssaj2013.01.0009.

Li, S.Y., Gu, X., Zhuang, J., An, T.T., Pei, J.B., Xie, H.T., Li, H., Fu, S.F., Wang, J.K., 2016. Distribution and storage of crop residue carbon in aggregates and its contribution to organic carbon of soil with low fertility. Soil Tillage Res. 155, 199-206. http://doi.org/10.1016/j.still.2015.08.009.

Liang, B., Lehmann, J., Solomon, D., Kinyangi, J., Grossman, J., O'Neill, B., Skjemstad, J.O., Thies, J., Luizao, F.J., Petersen, J., Neves, E.G., 2006. Black Carbon increases cation exchange capacity in soils. Soil Sci. Soc. Am. J. 70, 1719-1730. http://doi.org/10.2136/sssaj2005.0383.

Liang, Q., Chen, H., Gong, Y., Fan, M., Yang, H., Lal, R., Kuzyakov, Y., 2011. Effects of 15 years of manure and inorganic fertilizers on soil organic carbon fractions in a wheat-maize system in the North China Plain. Nutr. Cycl. Agroecosyst. 92,

https://doi.org/10.5194/egusphere-2026-1761
Preprint. Discussion started: 23 June 2026

687 21-33. http://doi.org/10.1007/s10705-011-9469-6.

688 Liu, J., Hu, F., Xu, C., Wang, Z., Ma, R., Zhao, S., Liu, G., 2021. Comparison of
689 different methods for assessing effects of soil interparticle forces on aggregate
690 stability. Geoderma 385. http://doi.org/10.1016/j.geoderma.2020.114834.

691 Liu, J., Wang, Z., Hu, F., Xu, C., Ma, R., Zhao, S., 2020. Soil organic matter and silt
692 contents determine soil particle surface electrochemical properties across a
693 long-term natural restoration grassland. Catena 190.
694 http://doi.org/10.1016/j.catena.2020.104526.

695 Liu, J.Y., Yang, Y.A., Zheng, Q.W., Su, X.M., Zhou, Z.C., 2022. Response of soil
696 aggregate stability and rill erodibility to soil electric field. Catena 215.
697 http://doi.org/10.1016/j.catena.2022.106338.

698 Lone, A.H., Najar, G.R., Ganie, M.A., Sofi, J.A., Ali, T., 2015. Biochar for
699 Sustainable Soil Health: A Review of Prospects and Concerns. Pedosphere 25,
700 639-653. http://doi.org/10.1016/s1002-0160(15)30045-x.

701 Lu, T., Wang, X., Du, Z., Wu, L., 2021. Impacts of continuous biochar application on
702 major carbon fractions in soil profile of North China Plain's cropland: In
703 comparison with straw incorporation. Agric. Ecosyst. Environ. 315.
704 http://doi.org/10.1016/j.agee.2021.107445.

705 Luo, C., Yang, J., Chen, W., Han, F., 2020. Effect of biochar on soil properties on the
706 Loess Plateau: Results from field experiments. Geoderma 369.
707 http://doi.org/10.1016/j.geoderma.2020.114323.

708 Ma, L.J., Lv, X.B., Cao, N., Wang, Z., Zhou, Z.G., Meng, Y.L., 2021a. Alterations of

https://doi.org/10.5194/egusphere-2026-1761
Preprint. Discussion started: 23 June 2026

soil labile organic carbon fractions and biological properties under different residue-management methods with equivalent carbon input. Appl. Soil Ecol. 161. http://doi.org/10.1016/j.apsoil.2020.103821.

Ma, N., Zhang, L., Zhang, Y., Yang, L., Yu, C., Yin, G., Doane, T.A., Wu, Z., Zhu, P., Ma, X., 2016. Biochar Improves Soil Aggregate Stability and Water Availability in a Mollisol after Three Years of Field Application. PLoS One 11, e0154091. http://doi.org/10.1371/journal.pone.0154091.

Ma, R., Hu, F., Liu, J., Zhao, S., 2021b. Evaluating the effect of soil internal forces on the stability of natural soil aggregates during vegetation restoration. J. Soils Sediments 21, 3034-3043. http://doi.org/10.1007/s11368-021-03011-z.

Ma, R.t., Guo, W., Hu, F.N., Xu, C.Y., Liu, G., Zhao, S.w., Zheng, F.l., 2022. Effects of soil internal forces on splash detachment and transport of aggregate fragments in Mollisols of Northeast China. Eur. J. Soil Sci. 73. http://doi.org/10.1111/ejss.13273.

Magill, A.H., Aber, J.D., 2000. Variation in soil net mineralization rates with dissolved organic carbon additions. Soil Biol. Biochem. 32, 597-601. http://doi.org/10.1016/s0038-0717(99)00186-8.

Meyer, W.L., Arp, P.A., Marsh, M., 1994. Cation exchange capacities of upland soils in eastern Canada. Can. J. Soil Sci. 74, 393-408. http://doi.org/10.4141/cjss94-053.

Okebalama, C.B., Marschner, B., 2023. Reapplication of biochar, sewage waste water, and NPK fertilizers affects soil fertility, aggregate stability, and carbon and

https://doi.org/10.5194/egusphere-2026-1761
Preprint. Discussion started: 23 June 2026

nitrogen in dry-stable aggregates of semi-arid soil. Sci. Total Environ. 866, 161203. http://doi.org/10.1016/j.scitotenv.2022.161203.

Pennell, K.D., Abriola, L.M., Boyd, S.A., 1995. Surface Area of Soil Organic Matter Reexamined. Soil Sci. Soc. Am. J. 59, 1012-1018. http://doi.org/10.2136/sssaj1995.03615995005900040008x.

Pituello, C., Dal Ferro, N., Francioso, O., Simonetti, G., Berti, A., Piccoli, I., Pisi, A., Morari, F., 2018. Effects of biochar on the dynamics of aggregate stability in clay and sandy loam soils. Eur. J. Soil Sci. 69, 827-842. http://doi.org/10.1111/ejss.12676.

Qiu, H., Liu, J., Boorboori, M.R., Li, D., Chen, S., Ma, X., Cheng, P., Zhang, H., 2023. Effect of biochar application rate on changes in soil labile organic carbon fractions and the association between bacterial community assembly and carbon metabolism with time. Sci. Total Environ. 855, 158876. http://doi.org/10.1016/j.scitotenv.2022.158876.

Quirk, J.P., 1994. Interparticle Forces: A Basis for the Interpretation of Soil Physical Behavior, Adv. Agron., pp. 121-183.

Rabot, E., Wiesmeier, M., Schlüter, S., Vogel, H.J., 2018. Soil structure as an indicator of soil functions: A review. Geoderma 314, 122-137. http://doi.org/10.1016/j.geoderma.2017.11.009.

Resurreccion, A.C., Moldrup, P., Tuller, M., Ferré, T.P.A., Kawamoto, K., Komatsu, T., De Jonge, L.W., 2011. Relationship between specific surface area and the dry end of the water retention curve for soils with varying clay and organic carbon

https://doi.org/10.5194/egusphere-2026-1761
Preprint. Discussion started: 23 June 2026

753 contents. Water Resour. Res. 47. http://doi.org/ 10.1029/2010wr010229.
754 Sheng, M.H., Ai, X.Y., Huang, B.C., Zhu, M.K., Liu, Z.Y., Ai, Y.W., 2023. Effects of
755 biochar additions on the mechanical stability of soil aggregates and their role in
756 the dynamic renewal of aggregates in slope ecological restoration. Sci. Total
757 Environ. 898, 165478. http://doi.org/10.1016/j.scitotenv.2023.165478.
758 Siedt, M., Schaffer, A., Smith, K.E.C., Nabel, M., Ross-Nickoll, M., van Dongen, J.T.,
759 2021. Comparing straw, compost, and biochar regarding their suitability as
760 agricultural soil amendments to affect soil structure, nutrient leaching, microbial
761 communities, and the fate of pesticides. Sci. Total Environ. 751, 141607.
762 http://doi.org/10.1016/j.scitotenv.2020.141607.
763 Šimanský, V., Igaz, D., Horák, J., Šurda, P., Kolenčík, M., Buchkina, N.P., Uzarowicz,
764 Ł., Juriga, M., Šrank, D., Pauková, Ž., 2018. Response of soil organic carbon and
765 water-stable aggregates to different biochar treatments including nitrogen
766 fertilization. J. Hydrol. Hydromech. 66, 429-436.
767 http://doi.org/10.2478/johh-2018-0033.
768 Stevenson, F.J., 1994. Humus chemistry: Genesis, composition, reactions. John Wiley,
769 New York.
770 Stewart, C.E., Paustian, K., Conant, R.T., Plante, A.F., Six, J., 2009. Soil carbon
771 saturation: Implications for measurable carbon pool dynamics in long-term
772 incubations. Soil Biol. Biochem. 41, 357-366.
773 http://doi.org/10.1016/j.soilbio.2008.11.011.
774 Sun, Q., Meng, J., Lan, Y., Shi, G.H., Yang, X., Cao, D.A.Y., Chen, W.F., Han, X.R.,

https://doi.org/10.5194/egusphere-2026-1761
Preprint. Discussion started: 23 June 2026

2021. Long-term effects of biochar amendment on soil aggregate stability and biological binding agents in brown earth. Catena 205. http://doi.org/10.1016/j.catena.2021.105460.

Tian, S., Zhu, B., Yin, R., Wang, M., Jiang, Y., Zhang, C., Li, D., Chen, X., Kardol, P., Liu, M., 2022. Organic fertilization promotes crop productivity through changes in soil aggregation. Soil Biol. Biochem. 165. http://doi.org/10.1016/j.soilbio.2021.108533.

Tuller, M., Or, D., 2005. Water films and scaling of soil characteristic curves at low water contents. Water Resour. Res. 41. http://doi.org/10.1029/2005wr004142.

Uchenna, O.S., Igbozurike, C.I., Nwachukwu, P.S., 2023. Biochar Application: An effective Measure in Improving the Fertility Status, Carbon Stock and Aggregate Stability of Eroded Soil. Turk. J. Agric. 11, 1276-1284. http://doi.org/10.24925/turjaf.v11i8.1276-1284.5655.

Wander, M.M., Traina, S.J., Stinner, B.R., Peters, S.E., 1994. Organic and Conventional Management Effects on Biologically Active Soil Organic Matter Pools. Soil Sci. Soc. Am. J. 58, 1130-1139. http://doi.org/10.2136/sssaj1994.03615995005800040018x.

Wang, D., Fonte, S.J., Parikh, S.J., Six, J., Scow, K.M., 2017. Biochar additions can enhance soil structure and the physical stabilization of C in aggregates. Geoderma 303, 110-117. http://doi.org/10.1016/j.geoderma.2017.05.027.

Wang, J., Fu, X., Sainju, U.M., Zhao, F.Z., 2018. Soil carbon fractions in response to straw mulching in the Loess Plateau of China. Biol. Fertil. Soils 54, 423-436.

https://doi.org/10.5194/egusphere-2026-1761
Preprint. Discussion started: 23 June 2026

http://doi.org/10.1007/s00374-018-1271-z.

Wang, K., Zhang, X., Zheng, J., Zhang, W., Yang, Z., Zhang, Q., Cai, J., Wang, X., 2024. Amended soils with weathered coal exhibited greater resistance to aggregate breakdown than those with biochar: From the viewpoint of soil internal forces. Soil Tillage Res. 244. http://doi.org/10.1016/j.still.2024.106244.

Wang, L.W., Ok, Y.S., Tsang, D.C.W., Alessi, D.S., Rinklebe, J., Masek, O., Bolan, N.S., Hou, D.Y., 2022. Biochar composites: Emerging trends, field successes and sustainability implications. Soil Use Manage. 38, 14-38. http://doi.org/10.1111/sum.12731.

Wei, Z., Zhao, X., Zhu, C., Xi, B., Zhao, Y., Yu, X., 2014. Assessment of humification degree of dissolved organic matter from different composts using fluorescence spectroscopy technology. Chemosphere 95, 261-267. http://doi.org/10.1016/j.chemosphere.2013.08.087.

Xu, C.Y., Li, H., Hu, F.N., Li, S., Liu, X.M., Li, Y., 2015. Non-classical polarization of cations increases the stability of clay aggregates: specific ion effects on the stability of aggregates. Eur. J. Soil Sci. 66, 615-623. http://doi.org/10.1111/ejss.12252.

Yagüe, M.R., Domingo-Olivé, F., Bosch-Serra, À.D., Poch, R.M., Boixadera, J., 2016. Dairy Cattle Manure Effects on Soil Quality: Porosity, Earthworms, Aggregates and Soil Organic Carbon Fractions. Land Degrad. Dev. 27, 1753-1762. http://doi.org/10.1002/ldr.2477.

Yang, C.D., Lu, S.G., 2021. Effects of five different biochars on aggregation, water

https://doi.org/10.5194/egusphere-2026-1761
Preprint. Discussion started: 23 June 2026

retention and mechanical properties of paddy soil: A field experiment of three-season crops. Soil Tillage Res. 205. http://doi.org/10.1016/j.still.2020.104798.

Yang, X., Meng, J., Lan, Y., Chen, W., Yang, T., Yuan, J., Liu, S., Han, J., 2017. Effects of maize stover and its biochar on soil CO 2 emissions and labile organic carbon fractions in Northeast China. Agric. Ecosyst. Environ. 240, 24-31. http://doi.org/10.1016/j.agee.2017.02.001.

Yu, Z., Zhang, J., Zhang, C., Xin, X., Li, H., 2017. The coupling effects of soil organic matter and particle interaction forces on soil aggregate stability. Soil Tillage Res. 174, 251-260. http://doi.org/10.1016/j.still.2017.08.004.

Yu, Z., Zheng, Y., Zhang, J., Zhang, C., Ma, D., Chen, L., Cai, T., 2020. Importance of soil interparticle forces and organic matter for aggregate stability in a temperate soil and a subtropical soil. Geoderma 362. http://doi.org/10.1016/j.geoderma.2019.114088.

Zhang, Q.Q., Song, Y.F., Wu, Z., Yan, X.Y., Gunina, A., Kuzyakov, Y., Xiong, Z.Q., 2020. Effects of six-year biochar amendment on soil aggregation, crop growth, and nitrogen and phosphorus use efficiencies in a rice-wheat rotation. J. Clean Prod. 242. http://doi.org/10.1016/j.jclepro.2019.118435.

Zhang, Q.Z., Du, Z.L., Lou, Y.L., He, X.H., 2015. A one-year short-term biochar application improved carbon accumulation in large macroaggregate fractions. Catena 127, 26-31. http://doi.org/10.1016/j.catena.2014.12.009.

Zhang, Y., Shengzhe, E., Wang, Y.A., Su, S.M., Bai, L.Y., Wu, C.X., Zeng, X.B., 2021.

https://doi.org/10.5194/egusphere-2026-1761
Preprint. Discussion started: 23 June 2026

Long-term manure application enhances the stability of aggregates and aggregate-associated carbon by regulating soil physicochemical characteristics. Catena 203. http://doi.org/10.1016/j.catena.2021.105342.

Zhang, Y.F., Dou, S., Ndzelu, B.S., Ma, R., Zhang, D.D., Zhang, X.W., Ye, S.F., Wang, H.R., 2022. Effects of returning corn straw and fermented corn straw to fields on the soil organic carbon pools and humus composition. Soil 8, 605-619. http://doi.org/10.5194/soil-8-605-2022.

Zhao, S.X., Ta, N., Li, Z.H., Yang, Y., Zhang, X., Liu, D., Zhang, A., Wang, X.D., 2018. Varying pyrolysis temperature impacts application effects of biochar on soil labile organic carbon and humic fractions. Appl. Soil Ecol. 123, 484-493. http://doi.org/10.1016/j.apsoil.2017.09.007.

https://doi.org/10.5194/egusphere-2026-1761
Preprint. Discussion started: 23 June 2026

863 **Table 1** Basic physicochemical properties of the soil

pH	Bulk density ($g\ cm^{3}$)	Organic carbon ($g\ kg^{-1}$)	Total nitrogen ($g\ kg^{-1}$)	Available phosphorus ($mg\ kg^{-1}$)	Available potassium ($mg\ kg^{-1}$)
7.53	1.33	9.02	0.82	20.79	165.52

864

865

https://doi.org/10.5194/egusphere-2026-1761
Preprint. Discussion started: 23 June 2026

866 **Table 2** Basic properties of biochar

Biochar	pH	C (%)	H (%)	O (%)	N (%)	H/C	O/C	SSA (m^2 g^{-1})	Ash (%)
Maize	6.30	32.67	0.92	11.72	0.48	0.03	0.36	14.48	7.51
Wheat	6.08	76.10	2.18	24.21	0.67	0.03	0.32	15.17	3.52

867

868

https://doi.org/10.5194/egusphere-2026-1761
Preprint. Discussion started: 23 June 2026

869 **Table 3** Soil electrochemical properties under biochar treatment for 180 days

Treatment	SCN (cmol(c) kg^{-1})	SSA (m^2 g^{-1})	σ_0 (c m^{-2})
CK	13.12 ±0.36e	32.23 ±2.42c	0.39 ±0.04a
M1	16.18 ±0.72d	40.63 ±7.67bc	0.39 ±0.08a
M3	17.50 ±0.14c	45.69 ±3.56b	0.37 ±0.03abc
M5	18.35 ±0.08b	49.94 ±0.57b	0.35 ±0.01abc
M10	18.72 ±0.03ab	61.58 ±7.24a	0.30 ±0.03c
W1	16.67 ±0.36d	42.26 ±7.04b	0.39 ±0.07ab
W3	17.50 ±0.09c	45.70 ±3.39b	0.37 ±0.03abc
W5	18.29 ±0.40b	47.85 ±5.43b	0.37 ±0.05abc
W10	19.21 ±0.16a	61.73 ±7.40a	0.30 ±0.04bc

870 Note: M1, M3, M5, M10, add 1%, 3%, 5%, 10% maize straw biochar; W1, W3, W5, W10, add
871 1%, 3%, 5%, 10% wheat straw biochar; CEC: cation exchange capacity, SSA: specific surface
872 area, σ_0: surface charge density; Values are means ± stand deviation (n = 3).

873

874

875

https://doi.org/10.5194/egusphere-2026-1761
Preprint. Discussion started: 23 June 2026

Table 4 Redundancy analysis of soil surface electrochemical properties and active carbon fractions after 180 and 365 days.

	Soil active carbon fractions	Explanation rate (%)	*F*	*P*
180 d	ROC	63.6	43.7	0.002
	DOC	1.7	1.2	0.322
	LFOC	1.5	1	0.37
	POC	1.7	1.2	0.348
365 d	POC	66.1	48.7	0.002
	DOC	0.5	0.4	0.614
	LFOC	0.4	0.3	0.762
	ROC	0.1	0.1	0.878

Note: ROC: readily oxidized organic carbon; DOC: dissolved organic carbon; LFOC: Light fraction organic carbon; POC: particulate organic carbon.

https://doi.org/10.5194/egusphere-2026-1761
Preprint. Discussion started: 23 June 2026

881 **Table 5** Changes in soil Hamaker constant under different treatments after 180 and

882 365 days.

Treatment	Hamaker（J）180 d	R^2	Hamaker（J）365 d	R^2
CK	$4.78\times10^{-20}\pm5.91\times10^{-21}$	0.82	$4.79\times10^{-20}\pm4.63\times10^{-21}$	0.90
M1	$6.01\times10^{-20}\pm6.05\times10^{-21}$	0.82	$8.89\times10^{-20}\pm7.27\times10^{-21}$	0.85
M3	$6.08\times10^{-20}\pm7.99\times10^{-21}$	0.73	$9.47\times10^{-20}\pm8.29\times10^{-21}$	0.83
M5	$6.06\times10^{-20}\pm7.71\times10^{-21}$	0.78	$9.78\times10^{-20}\pm6.28\times10^{-21}$	0.91
M10	$6.15\times10^{-20}\pm6.90\times10^{-21}$	0.78	$1.06\times10^{-19}\pm3.44\times10^{-21}$	0.98
W1	$4.96\times10^{-20}\pm5.95\times10^{-21}$	0.81	$7.38\times10^{-20}\pm7.57\times10^{-21}$	0.75
W3	$5.02\times10^{-20}\pm6.67\times10^{-21}$	0.75	$8.39\times10^{-20}\pm7.80\times10^{-21}$	0.79
W5	$5.19\times10^{-20}\pm6.08\times10^{-21}$	0.82	$8.73\times10^{-20}\pm3.78\times10^{-21}$	0.95
W10	$5.22\times10^{-20}\pm5.55\times10^{-21}$	0.84	$8.85\times10^{-20}\pm2.69\times10^{-21}$	0.98

883 Note: M1, M3, M5, M10, add 1%, 3%, 5%, 10% maize straw biochar; W1, W3, W5, W10, add

884 1%, 3%, 5%, 10% wheat straw biochar; Values are means ±stand deviation (n = 3).

885

886

https://doi.org/10.5194/egusphere-2026-1761
Preprint. Discussion started: 23 June 2026

Figure Captions

Figure 1 Experimental plot design. Note: W is wheat straw biochar and M is maize straw biochar; 0, 1, 3, 5, and 10 represent 0%, 1%, 3%, 5%, and 10% biochar additions, respectively; A, B, and C represent three replicates, respectively.

Figure 2 Effect of biochar addition on soil active organic carbon fractions after 180 days. M1, M3, M5, M10, add 1%, 3%, 5%, 10% maize straw biochar; W1, W3, W5, W10, add 1%, 3%, 5%, 10% wheat straw biochar.

Figure 3 Pearson correlation analysis between soil active carbon fractions and soil electrochemical properties after 180 and 365 days. * indicates significant correlation at the 0.05 level; ** indicates significant correlation at the 0.01 level; and *** indicates significant correlation at the 0.001 level.

Figure 4 Redundancy analysis of soil active carbon fractions and soil electrochemical properties after 180 and 365 days.

Figure 5 Electrostatic repulsive pressure between soil particles at an interparticle distance of 2 nm under different electrolyte concentrations after 180 and 365 days. M1, M3, M5, M10, add 1%, 3%, 5%, 10% maize straw biochar; W1, W3, W5, W10, add 1%, 3%, 5%, 10% wheat straw biochar.

Figure 6 Distributions of van der Waals attractive pressure and surface hydration repulsive pressure under biochar addition after 180 and 365 days. M1, M3, M5, M10, add 1%, 3%, 5%, 10% maize straw biochar; W1, W3, W5, W10, add 1%, 3%, 5%, 10% wheat straw biochar.

Figure 7 Net pressure of soil particles at 2 nm for different electrolyte concentrations under biochar addition after 180 and 365 days. M1, M3, M5, M10, add 1%, 3%, 5%, 10% maize straw biochar; W1, W3, W5, W10, add 1%, 3%, 5%, 10% wheat straw biochar.

Figure 8 Soil aggregate breaking strength (< 5 μm, < 10 μm) at different electrolyte concentrations under biochar addition after 180 days. M1, M3, M5, M10, add 1%, 3%, 5%, 10% maize straw biochar; W1, W3, W5, W10, add 1%, 3%, 5%, 10% wheat straw biochar.

Figure 9 Relationship between the net pressure at a 2 nm distance between soil particles and aggregate breaking strength under biochar addition after 180 and 365 days. M1, M3, M5, M10, add 1%, 3%, 5%, 10% maize straw biochar; W1, W3, W5, W10, add 1%, 3%, 5%, 10% wheat straw biochar.

https://doi.org/10.5194/egusphere-2026-1761
Preprint. Discussion started: 23 June 2026

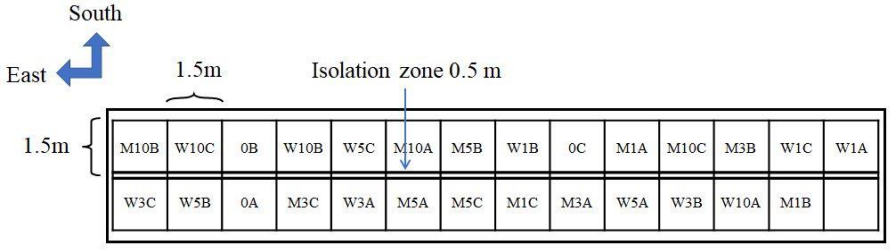

Figure 1 Experimental plot design.

https://doi.org/10.5194/egusphere-2026-1761
Preprint. Discussion started: 23 June 2026

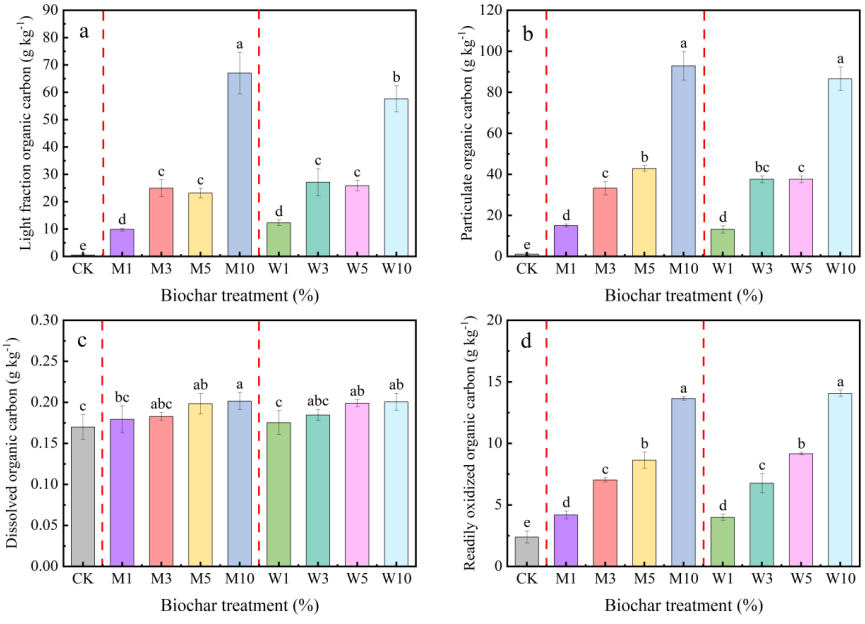

Fig. 2. Effect of biochar addition on soil active organic carbon fractions after 180 days.

https://doi.org/10.5194/egusphere-2026-1761
Preprint. Discussion started: 23 June 2026

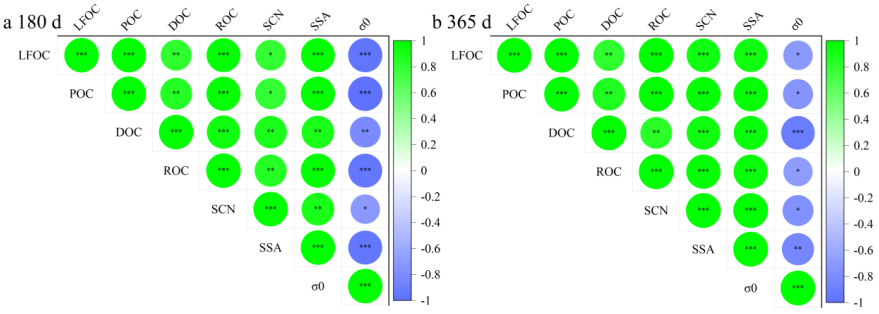

Fig. 3. Pearson correlation analysis between soil active carbon fractions and soil electrochemical properties after 180 and 365 days.

https://doi.org/10.5194/egusphere-2026-1761
Preprint. Discussion started: 23 June 2026

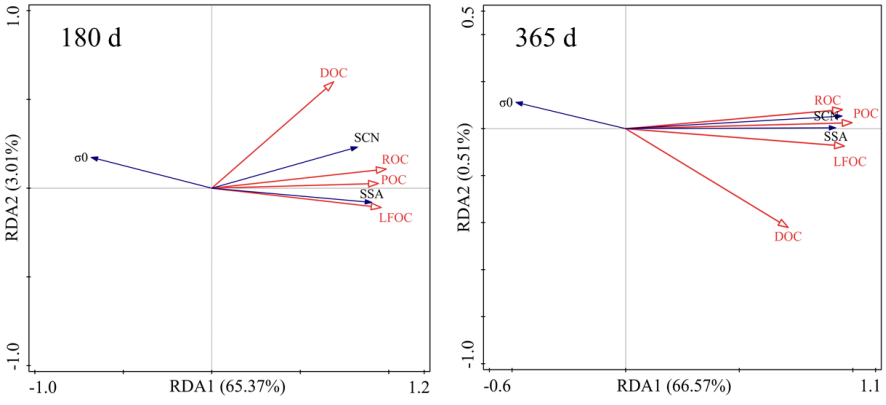

Fig. 4. Redundancy analysis of soil active carbon fractions and soil electrochemical properties after 180 and 365 days.

https://doi.org/10.5194/egusphere-2026-1761
Preprint. Discussion started: 23 June 2026

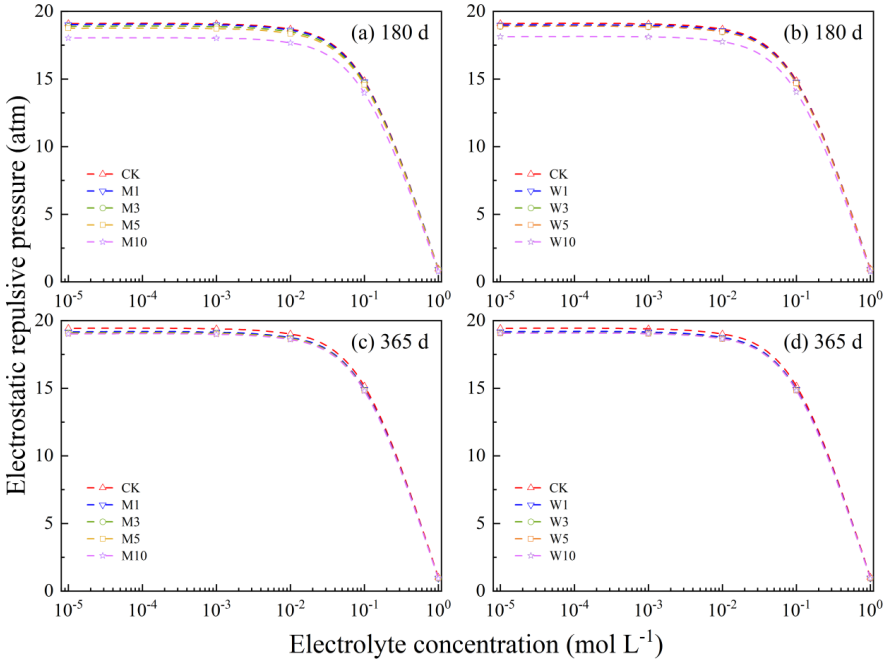

Fig. 5. Electrostatic repulsive pressure between soil particles at an interparticle distance of 2 nm under different electrolyte concentrations after 180 and 365 days.

https://doi.org/10.5194/egusphere-2026-1761
Preprint. Discussion started: 23 June 2026

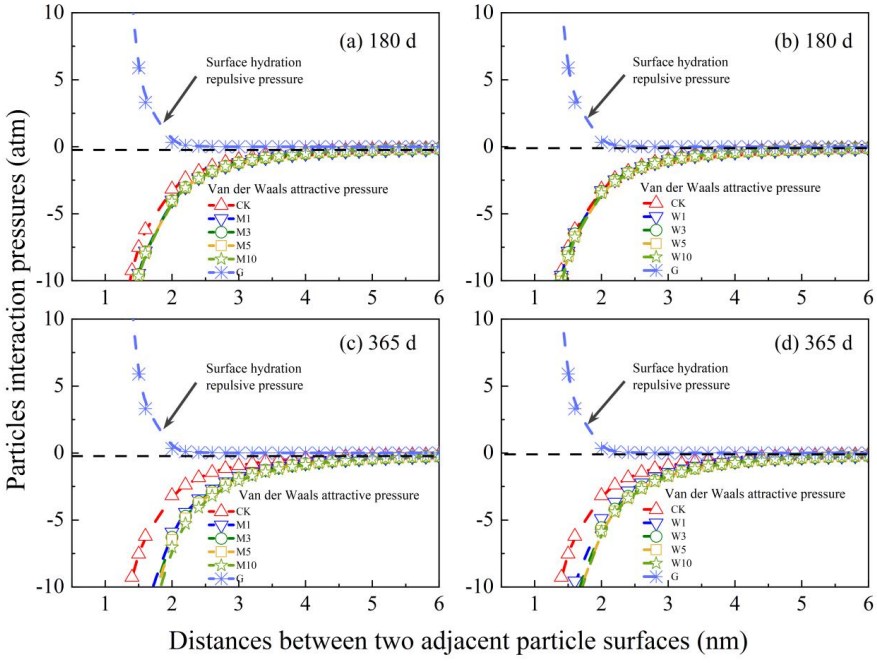

Fig. 6. Distributions of van der Waals attractive pressure and surface hydration repulsive pressure under biochar addition after 180 and 365 days.

https://doi.org/10.5194/egusphere-2026-1761
Preprint. Discussion started: 23 June 2026

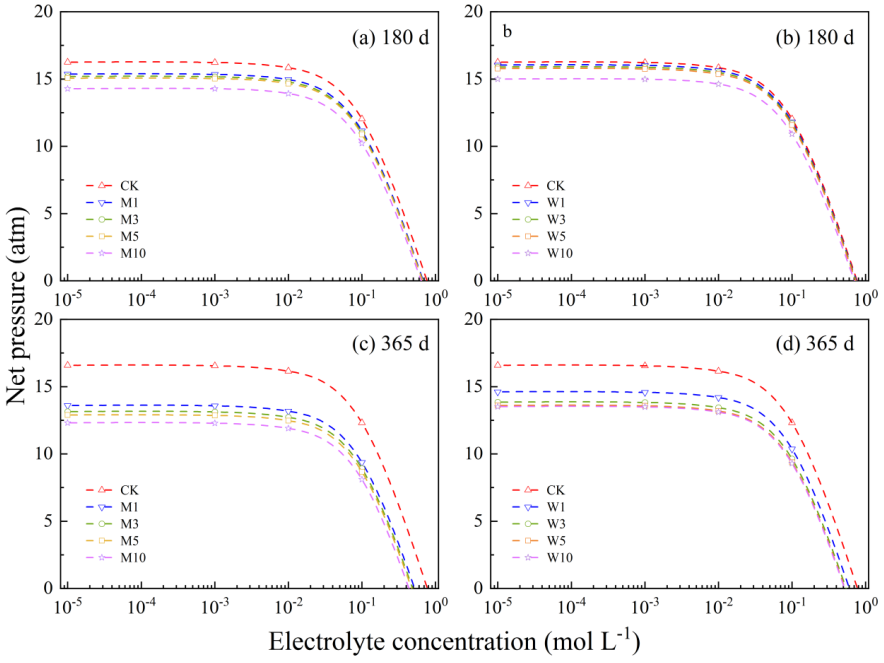

Fig. 7. Net pressure of soil particles at 2 nm for different electrolyte concentrations under biochar addition after 180 and 365 days.

https://doi.org/10.5194/egusphere-2026-1761
Preprint. Discussion started: 23 June 2026

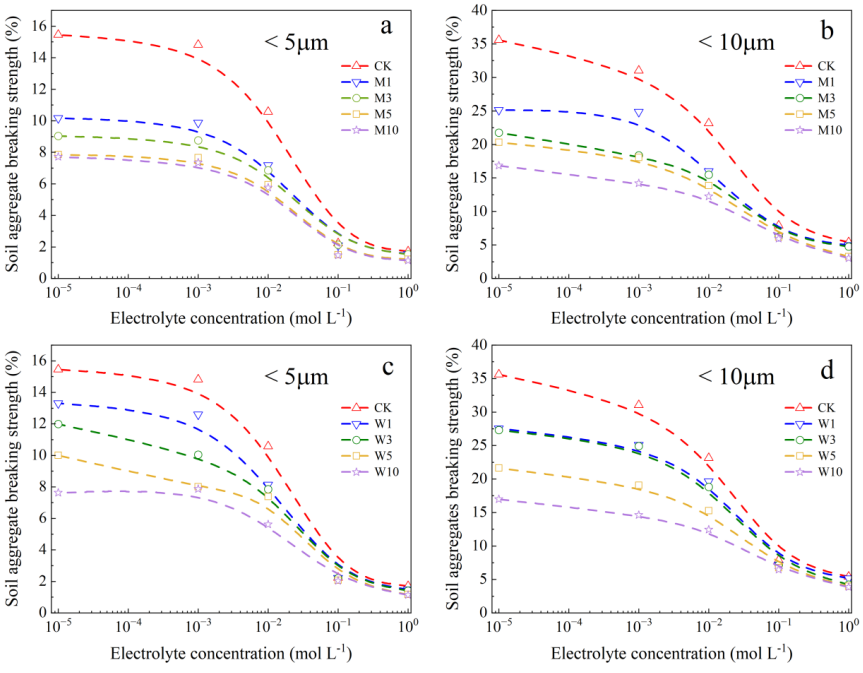

Fig. 8. Soil aggregate breaking strength (< 5 μm, < 10 μm) at different electrolyte concentrations under biochar addition after 180 days.

https://doi.org/10.5194/egusphere-2026-1761
Preprint. Discussion started: 23 June 2026

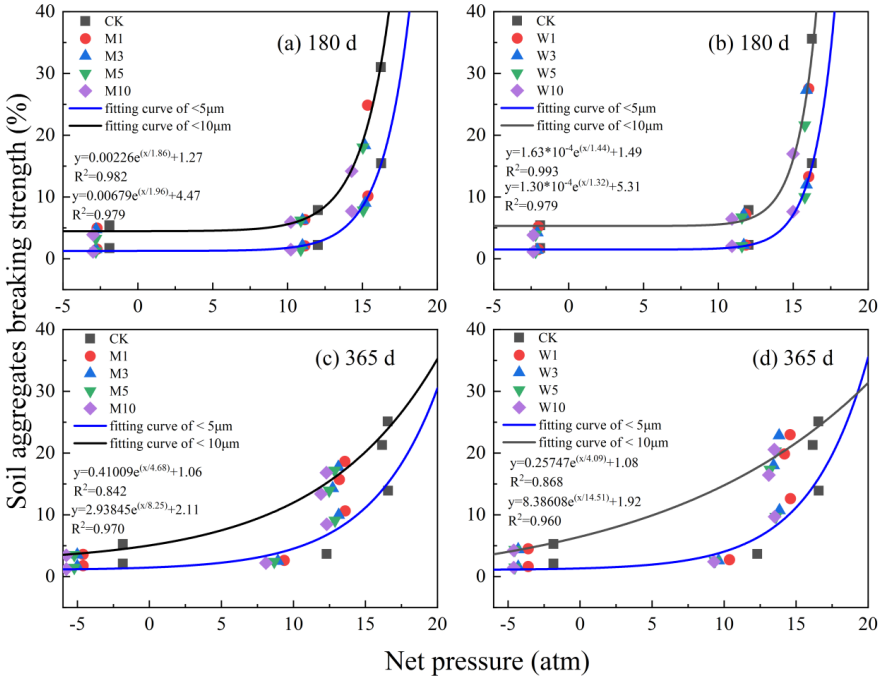

Fig. 9. Relationship between the net pressure at a 2 nm distance between soil particles and aggregate breaking strength under biochar addition after 180 and 365 days.